Processing of fullerene-single wall carbon nanotube complex for bulk heterojunction photovoltaic cells

Cheng Li and Somenath Mitra[a)]
Department of Chemistry and Environmental Science, New Jersey Institute of Technology, Newark, New Jersey 07102, USA

(Received 24 September 2007; accepted 1 December 2007; published online 19 December 2007)

A fullerene-single wall carbon nanotube (C_{60}-SWCNT) complex is used as a component of the photoactive layer in bulk heterojunction photovoltaic cells. This complex synthesized by microwave-assisted reaction takes advantage of the electron accepting feature of C_{60} and the high electron transport capability of SWCNTs. In this paper, quantum efficiency enhancement by increasing light absorption and by bringing about appropriate morphological rearrangements via solvent vapor treatment and thermal annealing is presented. The optimum combination of these steps led to an increase in efficiency by as much as 87.5%. © *2007 American Institute of Physics*. [DOI: 10.1063/1.2827189]

Among donor-acceptor type polymer photovoltaic cells (PVCs), the most promising material combination is poly(3-hexylthiophene) (P3HT) and the soluble fullerene derivative (6,6)-phenyl C_{61}-butyric acid methyl ester (PCBM).[1] Although PCBM can form better films and has higher electron mobility than fullerene (C_{60}), it is intrinsically expensive than the latter. On the other hand, C_{60} is a stronger electron acceptor and is more efficient in charge separation than PCBM.[2] Single wall carbon nanotubes (SWCNTs) are known to be excellent electron transporters and have been used in PVCs.[3] We have recently reported the synthesis of a C_{60}-SWCNT complex via a microwave induced reaction.[4] A P3HT:C_{60}-SWCNT composite was used to fabricate bulk heterojunction PVCs. The efficiency of such PVCs can be improved by increasing light absorption and by more efficient charge separation and transport.[1] Postproduction thermal treatment has been shown to improve efficiency due to controlled phase separation,[5,6] crystallization of the polymer, and suitable rearrangement of its chain structure.[7,8] Solvent vapor annealing, which was employed to improve regularity and order in thin films of block copolymers,[9,10] has recently been shown to improve performance of P3HT:PCBM photovoltaic cells.[11,12] The relatively large C_{60}-SWCNT (several hundreds of nanometers to micron scale) tends to form a composite with large heterogeneous structures, so optimizing film morphology plays an important role. We report in this letter the efficiency improvement of our P3HT:C_{60}-SWCNT PVCs by the combination of solvent and thermal annealings.

PVCs were fabricated on indium tin oxide (ITO) coated glass substrates (8–12 Ω/□). Poly(ethylenedioxy)-thiophene:poly(styrene)sulfonate (PEDOT:PSS) (Baytron P, H.C. Stark, Inc.) was spin coated onto cleaned substrates to obtain a 80–85 nm layer and dried at 115 °C for 15 min in an oven. The preparation of the C_{60}-SWCNT complex has been described elsewhere.[4] The photoactive composite was prepared by blending P3HT with the C_{60}-SWCNT complex at 1:1 weight ratio in a 50:50 mixture of toluene and dichlorobenzene. The composite solution was spin coated on top of the PEDOT:PSS layer to produce an active layer ~80 nm thickness. The freshly coated films were either dried in air or subjected to toluene solvent annealing for various times (1, 5, and 20 min) in a sealed glass Petri dish. A 100 nm thick aluminum (Al) cathode layer was thermally deposited using a shadow mask at a vacuum level better than 2×10^{-6} torr. The active cell area is approximately 0.16 cm^2, defined by the intersection of ITO and Al electrodes.

Current density-voltage (*J-V*) characteristics under simulated solar irradiation (95 mW/cm^2) were measured in air using a Newport 150 W solar simulator and a Keithley 2400 source-measuring unit, before and after thermal annealing (120 °C, 10 min) in a nitrogen-filled glove box. Thin films of P3HT:C_{60}-SWCNT prepared on cleaned glass substrates were characterized by UV-visible absorption spectroscopy and atomic force microscopy (AFM) using an HP 845 UV-visible absorption spectrophotometer and a Digital Instrument Nanoscope®IIIa scanning probe microscope, respectively.

Figure 1 shows UV-visible absorption spectra of P3HT:C_{60}-SWCNT films measured after solvent annealing for different lengths of times. The integrated visible absorption was defined as the area under the spectra in the range of 380–780 nm. As compared to the as-deposited film 1, sol-

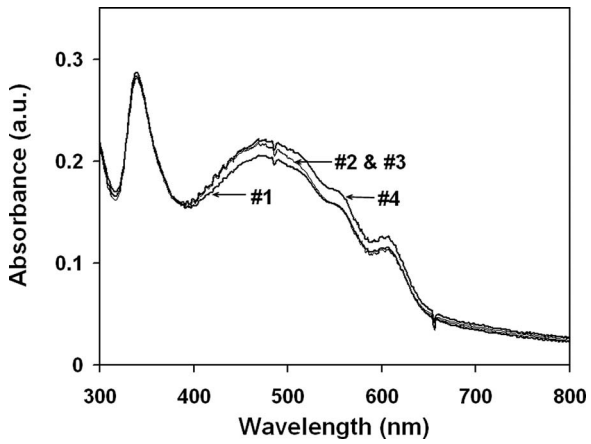

FIG. 1. UV-visible absorption spectra of P3HT:C_{60}-SWCNT composite films without solvent vapor annealing (1) and with solvent vapor annealing for 1 min (2), 5 min (3), and 20 min (4).

a)Author to whom correspondence should be addressed. Electronic mail: somenath.mitra@njit.edu.

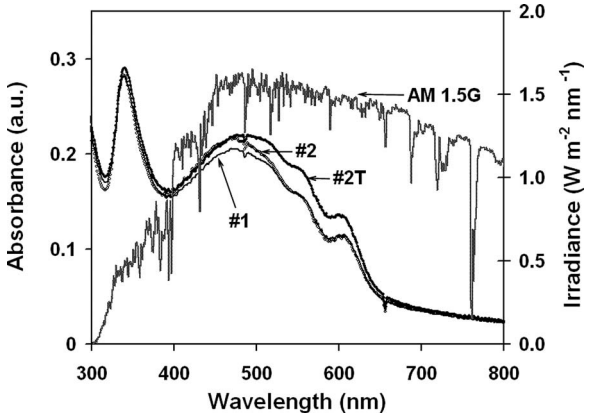

FIG. 2. UV-visible absorption spectra of P3HT:C_{60}-SWCNT film after 1 min solvent annealing (2) followed by subsequent thermal annealing (2*T*). Also shown in the figure are the absorption spectrum of the as-deposited film (1) and the AM 1.5G solar irradiance spectrum.

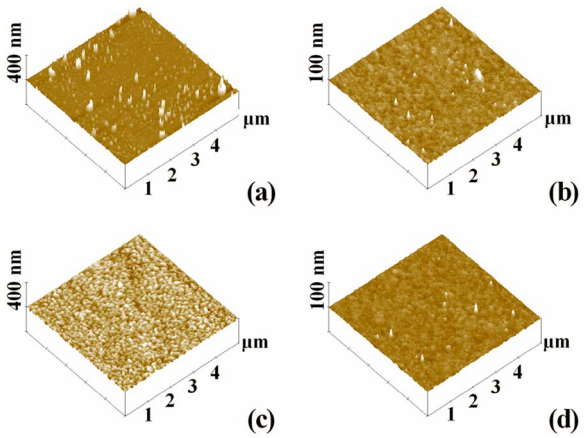

FIG. 3. (Color online) AFM images of P3HT:C_{60}-SWCNT composite films. (a) Film 1 (no solvent annealing), (b) film 1 after thermal annealing, (c) film 2 (1 min solvent annealed), and (d) film 2 after thermal annealing. Note that the data scale for images (a) and (c) is 0–200 nm, whereas for (b) and (d), it is 0–50 nm.

vent vapor treated films showed increased absorption without any shift of the absorption peak (~468 nm). This was different from what has been reported for P3HT:PCBM films, where a clear redshift was observed after solvent vapor treatment.[12] Similar to the P3HT:PCBM films, the absorption associated with fullerene (indicated by absorption peaks at ~340 nm) in P3HT:C_{60}-SWCNT films remained unchanged. While solvent annealing for 1 and 5 min induced absorption enhancement in the blue-green region (400–530 nm), increasing the annealing time resulted in higher absorption over the entire visible range.

Figure 2 shows UV-visible absorption spectra of film 2 before and after subsequent thermal treatment. It is evident that thermal annealing resulted in increased optical absorption and a redshift of the absorption peak (from 468 to 484 nm) with a better match to the solar spectrum, which are indicative of a more ordered polymer structure.[13] Similar changes were also observed on other thermally annealed films and were consistent with what has been reported in the literature.[13–15] The light absorption in films pretreated with solvent vapor for 1, 5, and 20 min were 3.6%, 6.2%, and 7.8% higher than that of film 1 which was not solvent annealed. As compared to the untreated film, the ones that had undergone both forms of annealing showed an increase in optical absorption, which could be as high as 14.4%.

Figure 3 shows AFM images of the films 1 and 2 before and after thermal annealing. The as-deposited film [Fig. 3(a)] was featureless with numerous spikes as high as ~100 nm. Solvent vapor was able to penetrate into the film during the annealing process to induce structural rearrangement.[10] After a short period of toluene vapor annealing, phase separation between P3HT and C_{60}-SWCNT was prominent, indicated by relatively uniform nanostructures with approximate domain size of around 20 nm [Fig. 3(c)]. After thermal annealing, both films became smoother with roughly the same average surface roughness R_a (~0.7 nm). For film 1, the formation of a uniform polymer phase was accompanied by reduced peak-to-valley height from ~100 to ~22 nm. The major change on film 2 was the growth of domains of uniform phase separation.

Photovoltaic parameters for PVCs with solvent annealing times of 0 (cell A), 1 (cell B), 5 (cell C), and 20 min (cell D) were extracted from their *J-V* curves and are listed in Table I. As compared to the control cell A, exposure of the active layer to toluene vapor for 1 min (cell B) resulted in a slight increase in the short-circuit current density (J_{SC}) from 1.75 to 1.90 mA/cm^2, and an increase in the fill factor (FF) from 43.3% to 45.5%. The open-circuit voltage (V_{OC}) remained unchanged. As a result, the power conversion efficiency (η) improved from 0.40% to 0.46%. This improvement may be attributed to simultaneous increase in optical absorption (Fig. 1) and in hole transport efficiency due to a more ordered polymer structure [Fig. 3(c)]. Solvent annealing for longer times (cells C and D) resulted in the decrease in cell efficiencies, even lower than that of control cell A. Analysis of the *J-V* curves in dark revealed that the reverse leakage currents measured at −2 V for cell C (2.86 mA/cm^2) and cell D (6.50 mA cm^{-2}) were much higher than those for cell A (0.77 mA/cm^2) and cell B (0.78 mA/cm^2). Higher leakage current resulted in lower collection efficiency which was indicated by the lower fill factors. It is also possible that some trapped solvent led to slower charge transport and higher probability of electron-hole recombination, leading to reduced cell efficiency. In general, for the P3HT:C_{60}-SWCNT system, although solvent annealing improved absorption by as much as 8.1%, it does not appear to be an effective method for increasing overall cell efficiency.

Improvement in performance after thermal annealing was quite evident for all the cells. However, this enhancement was more prominent on cells with previous solvent treatment. For example, the efficiency of cell C nearly tripled and that of cell D was more than doubled, while the efficiency of cell A increased by only 30%. The dramatic performance enhancement after thermal annealing for solvent treated cells resulted from overall improvement in V_{OC}, FF, and especially J_{SC}. The highest J_{SC} (2.70 mA/cm^2) and the largest percentage increase in J_{SC} (92.6%) occurred for cell C. More importantly, under the same thermal annealing condition, all solvent annealed cells showed efficiencies higher than the control cell A. Notably, the efficiency of cell B was 87.5% higher than the as-fabricated cell A. This enhancement is rather dramatic and demonstrates the importance of the combination of solvent and thermal annealing. As mentioned before, this is particularly relevant to the P3HT:C_{60}-SWCNT system. For example, as compared to only thermal annealing, this combination showed a barely

TABLE I. Photovoltaic parameters for P3HT:C_{60}-SWCNT cells under 95 mW/cm^2 simulated solar irradiation measured after device fabrication and after subsequent thermal annealing. Active layers in these cells were either as-deposited or exposed to toluene solvent vapor for a specified time (t_{SA}).

	As-fabricated				Thermally annealed			
Cell (t_{SA})	V_{OC} (V)	J_{SC} (mA/cm^2)	FF (%)	η (%)	V_{OC} (V)	J_{SC} (mA/cm^2)	FF (%)	η (%)
A								
(0 min)	0.500	1.75	43.3	0.40	0.532	2.52	37.1	0.52%
B								
(1 min)	0.506	1.90	45.5	0.46	0.541	2.69	49.2	0.75%
C								
(5 min)	0.429	1.40	38.4	0.24	0.527	2.70	47.4	0.71%
D								
(20 min)	0.412	1.46	36.9	0.23	0.529	2.54	42.5	0.60%

10% enhancement in efficiency for the P3HT:PCBM system while 44% in the present one.

For the P3HT:PCBM PVCs, it has been reported that subsequent thermal annealing had little effect on the absorption of slow-grown[11] or vapor treated[12] films. However, for the P3HT:C_{60}-SWCNT films, subsequent thermal annealing not only enhanced absorption but also caused a redshift of the absorption peak. This is an indication of higher degree of structural ordering of the polymer phase.[5] It is well known that appropriate reordering of the polymer enhances hole mobility,[16] while the phase separation and growth of PCBM domains promote electron transport.[5] In previously published studies, especially pertaining to the P3HT:PCBM PVCs, thermal annealing is known to reorder P3HT domains via interchain actions[17] and molecular diffusion of the PCBM phase out of the polymer matrix.[5] For the P3HT:C_{60}-SWCNT system, the phase separation was observed during solvent annealing. However, the average domain size of the C_{60}-SWCNT phase was not large enough to promote the formation of enough percolation pathways for efficient electron transport. As a high energy process, thermal annealing was more effective in providing the driving force needed for enhanced ordering of polymer structure and the interconnection of C_{60}-SWCNT domains. These led to more efficient transport of photogenerated charge carriers. These effects were more significant for PVCs pretreated with solvent vapor for longer periods of time (cells C and D). The calculated reverse leakage current reduced to 0.26 mA/cm^2 after thermal annealing for both cells, indicating a smaller number of defects in the active layer. Morphological change of the active layer also played a significant role. A smoother surface on thermally annealed films (Fig. 3) provided a better contact between the active layer and the cathode for more efficient electron collection. These factors contributed to the dramatic increases in J_{SC} and FF on cells C and D. Based on these observations, it is evident that an optimum combination of solvent and thermal annealings is an effective method for enhancing quantum efficiency of the P3HT:C_{60}-SWCNT system.

In conclusion, the morphology and the absorption characteristics for relatively large C_{60}-SWCNT heterogeneous structures could be effectively altered by means of solvent vapor annealing of the active layer followed by thermal treatment. Thermal annealing of solvent pretreated films significantly improved cell performance due to enhanced absorption and optimum phase separation, with a 87.5% efficiency enhancement as compared to a control cell without any annealing. The combination of solvent and thermal annealings is clearly the optimum strategy to achieve high efficiency with P3HT:C_{60}-SWCNT PVCs.

The authors thank the US Army ARDEC for financial support of this work. Ms. Yuhong Chen is acknowledged for her help in the synthesis of the C_{60}-SWCNT complex.

[1] R. A. J. Janssen, J. C. Hummelen, and N. S. Sariciftci, MRS Bull. **30**, 33 (2005).
[2] M. Al-Ibrahim, H.-K. Roth, M. Schroedner, A. Konkin, U. Zhokhavets, G. Gobsch, P. Scharff, and S. Sensfuss, Org. Electron. **6**, 65 (2005).
[3] E. Kymakis, I. Alexandrou, and G. A. J. Amaratunga, J. Appl. Phys. **93**, 1764 (2003).
[4] C. Li, Y. Chen, Y. Wang, Z. Iqbal, M. Chhowalla, and S. Mitra, J. Mater. Chem. **17**, 2407 (2007).
[5] D. Chirvase, J. Parisi, J. C. Hummelen, and V. Dyakonov, Nanotechnology **15**, 1317 (2004).
[6] Y. Kim, S. A. Choulis, J. Nelson, D. D. C. Bradley, S. Cook, and J. R. Durrant, Appl. Phys. Lett. **86**, 063502 (2005).
[7] N. Camaioni, G. Ridolfi, G. Casalbore-Miceli, G. Possamai, and M. Maggini, Adv. Mater. (Weinheim, Ger.) **14**, 1735 (2002).
[8] U. Zhokhavets, T. Erb, H. Hoppeb, G. Gobsch, and N. S. Sariciftci, Thin Solid Films **496**, 679 (2006).
[9] S. Niu and R. F. Saraf, Macromolecules **36**, 2428 (2003).
[10] K. A. Cavicchi, K. J. Berthiaume, T. P. Russell, Polymer **46**, 11635 (2005).
[11] G. Li, V. Shrotriya, J. Huang, Y. Yao, T. Moriarty, K. Emery, and Y. Yang, Nat. Mater. **4**, 864 (2005).
[12] Y. Zhao, Z. Xie, Y. Qu, Y. Geng, and L. Wang, Appl. Phys. Lett. **90**, 043504 (2007).
[13] V. Dyakonov, Appl. Phys. A: Mater. Sci. Process. **79**, 21 (2004).
[14] G. Li, V. Shrotriya, Y. Yao, and Y. Yang, J. Appl. Phys. **98**, 043704 (2005).
[15] K. Inoue, R. Ulbricht, P. C. Madakasira, W. M. Sampson, S. Lee, J. Gutierrez, J. Ferraris, and A. A. Zakhidov, Synth. Met. **154**, 41 (2005).
[16] Z. Bao, A. Dodabalapur, and A. J. Lovinger, Appl. Phys. Lett. **69**, 4108 (1996).
[17] P. J. Brown, D. S. Thomas, A. Kohler, J. Wilson, J. S. Kim, C. Ramsdale, H. Sirringhaus, and R. H. Friend, Phys. Rev. B **67**, 064203 (2003).